

See discussions, stats, and author profiles for this publication at: <https://www.researchgate.net/publication/243347775>

# Ab initio MO–CI based quantum master equation approach: Exciton dynamics of weakly and strongly coupled J-type aggregates

ARTICLE *in* SYNTHETIC METALS · NOVEMBER 2009

Impact Factor: 2.25 · DOI: 10.1016/j.synthmet.2009.09.023

CITATIONS

2

READS

25

7 AUTHORS, INCLUDING:



**Ryohei Kishi**

Osaka University

110 PUBLICATIONS 1,955 CITATIONS

SEE PROFILE



**Masayoshi Nakano**

Osaka University

337 PUBLICATIONS 4,793 CITATIONS

SEE PROFILE

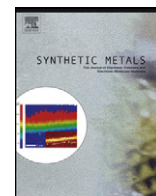


**Kyohei Yoneda**

Nara National College of Technology

42 PUBLICATIONS 599 CITATIONS

SEE PROFILE



# Ab initio MO–CI based quantum master equation approach: Exciton dynamics of weakly and strongly coupled J-type aggregates

Ryohei Kishi\*, Masayoshi Nakano\*, Takuya Minami, Hitoshi Fukui, Hiroshi Nagai, Kyohei Yoneda, Hideaki Takahashi

Department of Materials Engineering Science, Graduate School of Engineering Science, Osaka University, Toyonaka, Osaka 560-8531, Japan

## ARTICLE INFO

### Article history:

Received 26 July 2008

Received in revised form

12 September 2009

Accepted 14 September 2009

Available online 4 November 2009

### Keywords:

Exciton

Polarization

Ab initio MO method

Quantum master equation

## ABSTRACT

In order to investigate the time evolutions of electron and hole distributions in weakly and strongly coupled  $H_2$  dimer models, we employ a novel dynamic exciton expression derived from the exciton density matrices calculated by the quantum master equation combined with the ab initio molecular orbital (MO)–configuration interaction (CI) method. The oscillation of exciton distribution over the monomers is observed in case of small inter-monomer distance, where the coupled dipole approximation is invalid. The result originates in the covalent character of inter-monomer interaction in the first excited state, i.e., delocalized character of LUMO distribution.

© 2009 Elsevier B.V. All rights reserved.

## 1. Introduction

Coherent and incoherent (relaxation) dynamics of exciton (electron–hole pair), e.g., exciton migration and recurrence motion, in molecular aggregates and supermolecular systems is one of the recent hot topics in dynamical quantum features of biological, photonics and optoelectronics systems [1–8]. On the theoretical side, the Förster's formula [9] has been widely used to discuss the transition probability of singlet–singlet resonance exciton energy transfer from one to another molecules. In view of detailed analysis of exciton dynamics, several approaches for quantum dynamics [3,10–16], such as, the reduced density matrix (RDM) approach, have been developed recently, where the equation of motion of exciton density is solved numerically. Additionally, modeling of exciton states is also important aspect. In the Frenkel exciton model [17] which is widely used for the description of molecular exciton, a pair of electron and hole moves within each molecule under a constraint of taking the same position with each other. The dipole–dipole coupling is often employed in order to approximate the intermolecular interaction between very weakly coupled molecules. There have been several approaches improving the dipole–dipole approximation within the Coulomb interaction [18–23]. Such treatments have achieved great suc-

cesses in describing the exciton states of molecular aggregates with weak interactions, e.g., van der Waals interactions. On the other hand, exciton dynamics of strongly coupled aggregates and supermolecules, e.g., charge transfer interactions, and in supermolecular systems with extended electron delocalization cannot be described when the Coulomb interaction is not the dominant part in the whole inter-monomer interaction.

In previous papers [13,16], we have proposed a novel exciton description based on the ab initio molecular orbital (MO)–configuration interaction (CI) method combined with the quantum master equation method (MQME) to eliminate these defects. Particularly, a newly defined dynamic exciton expression can reproduce the time evolution of system polarization, which represents the coherent exciton dynamics [16]. In this contribution, we examine the intra- and inter-monomer exciton dynamics of electron–hole pair in weakly and strongly coupled aggregates using simple J-aggregate models composed of  $H_2$  molecules. We compare the results for exciton state models with those calculated by the dipole–dipole approximation in order to clarify the advantage and the applicable target of the present scheme.

## 2. Calculation methods

Since details of the MQME approach is described in Ref. [16], we here briefly provide the concept of this approach combined with the new dynamic exciton expression. The time-evolution of exciton RDM is obtained using the singlet adiabatic exciton state basis

\* Corresponding author. Tel.: +81 6 6850 6265; fax: +81 6 6850 6268.

E-mail addresses: [rkishi@cheng.es.osaka-u.ac.jp](mailto:rkishi@cheng.es.osaka-u.ac.jp) (R. Kishi), [mnaka@cheng.es.osaka-u.ac.jp](mailto:mnaka@cheng.es.osaka-u.ac.jp) (M. Nakano).

**Table 1**

Transition energy ( $E_2$ ) and transition dipole moment ( $\mu_{12}^x$ ) between the ground and first dipole allowed excited states calculated by the SCI, dipole-dipole approximation, and full-CI methods as well as the CI coefficients of HOMO (H)-LUMO (L) single excitation configuration for each model. The SCI monomer parameters are employed for the dipole-dipole approximation.

		H <sub>2</sub> monomer	H <sub>2</sub> dimer	
			$R=0.7389 \text{ \AA}$	$R=3.0 \text{ \AA}$
This work (SCI)	$E_2 \text{ (cm}^{-1}\text{)}$	208415	150432	205639
	$\mu_{12}^x \text{ (D)}$	−3.343	5.338	4.719
	CI coefficient (H → L)	1.000	0.998	0.793
Dipole-dipole	$E_2 \text{ (cm}^{-1}\text{)}$	(208415)	69262	204289
	$\mu_{12}^x \text{ (D)}$	(−3.343)	6.345	4.774
Full-CI	$E_2 \text{ (cm}^{-1}\text{)}$	212907	154378	210686
	$\mu_{12}^x \text{ (D)}$	−2.946	−4.677	4.181
	CI coefficient (H → L)	1.000	0.990	0.781

$$\{|\alpha\rangle\} \equiv \{|\Psi_\alpha\rangle\}:$$

$$|\alpha\rangle = \sum_i^N |i\rangle \langle i|\alpha\rangle = \sum_i^N |i\rangle C_{i\alpha}. \quad (1)$$

Here, the singly excitation configurations from occupied MO  $a$  to virtual MO  $r$ ,  $\{|i\rangle \equiv |\Psi_a^r\rangle\}$ , are assumed to compose the one-exciton bases, and the exciton vacuum state  $|1\rangle$  corresponds the Hartree-Fock (HF) ground configuration. The expansion coefficients,  $\{C_{i\alpha}\}$  (referred to as CI coefficients) are obtained by the ab initio singly excitation CI (SCI) calculation using the Gaussian 03 program package [24].

Assuming the weak interaction between exciton and phonon bath states, we derive the quantum master equation for the system RDM ( $\rho_{\alpha\beta}$ ) using the adiabatic state basis in the Born-Markov approximation [12,25]. The system density matrices are converted

to those using the one-exciton basis by  $\rho_{ij}^{\text{ex}}(t) = \sum_{\alpha\beta}^M C_{i\alpha}^* C_{j\beta} \rho_{\alpha\beta}(t)$ .

We define the polarization density  $\rho_{\text{pol}}(\mathbf{r}, t)$  as the density differ-

ence between the one-electron reduced density at time  $t$  [ $\rho(\mathbf{r}, t)$ ] and that at the initial state:

$$\begin{aligned} \rho_{\text{pol}}(\mathbf{r}, t) &\equiv \rho(\mathbf{r}, t) - d_{11}(\mathbf{r}) \\ &= \sum_{i=2} [d_{ii}(\mathbf{r}) - d_{11}(\mathbf{r})] \rho_{ii}(t) + 2 \sum_{i=2} d_{1i}(\mathbf{r}) \rho_{1i}^{\text{real}}(t) \\ &\quad + 2 \sum_{i < j (i,j \neq 1)} d_{ij}(\mathbf{r}) \rho_{ij}^{\text{real}}(t), \end{aligned} \quad (2)$$

where  $d_{ij}(\mathbf{r})$  indicates the reduced one-electron density matrices using the one-exciton basis  $\{|i\rangle\}$  including the exciton vacuum state  $|1\rangle$ . Using the occupied  $\{\psi_a(\mathbf{r}), \psi_b(\mathbf{r}), \dots\}$  and virtual  $\{\psi_r(\mathbf{r}), \psi_s(\mathbf{r}), \dots\}$  MOs, and the relationship:  $\rho_{\text{pol}}(\mathbf{r}, t) \equiv \rho_{\text{elec}}(\mathbf{r}, t) - \rho_{\text{hole}}(\mathbf{r}, t)$ , we partition Eq. (2) into  $\rho_{\text{elec}}(\mathbf{r}, t)$  and  $\rho_{\text{hole}}(\mathbf{r}, t)$  as,

$$\begin{aligned} \rho_{\text{elec}}(\mathbf{r}, t) &= \sum_{i(a \rightarrow r)=2} \left[ \rho_{ii}(t) |\psi_r(\mathbf{r})|^2 + \sqrt{2} \psi_a(\mathbf{r}) \psi_r(\mathbf{r}) \rho_{1i}^{\text{real}}(t) \right. \\ &\quad \left. + 2 \sum_{j(a \rightarrow s)(>i)} \psi_r(\mathbf{r}) \psi_s(\mathbf{r}) \rho_{ij}^{\text{real}}(t) \right], \end{aligned} \quad (3)$$

and,

$$\begin{aligned} \rho_{\text{hole}}(\mathbf{r}, t) &= \sum_{i(a \rightarrow r)=2} \left[ \rho_{ii}(t) |\psi_a(\mathbf{r})|^2 - \sqrt{2} \psi_a(\mathbf{r}) \psi_r(\mathbf{r}) \rho_{1i}^{\text{real}}(t) \right. \\ &\quad \left. + 2 \sum_{j(b \rightarrow r)(>i)} \psi_a(\mathbf{r}) \psi_b(\mathbf{r}) \rho_{ij}^{\text{real}}(t) \right] \end{aligned} \quad (4)$$

Although the electron and hole densities should take values between 0 and 1 by definition,  $\rho_{\text{elec}}(\mathbf{r}, t)$  and  $\rho_{\text{hole}}(\mathbf{r}, t)$  of Eqs. (3) and (4) could take negative values for some positions  $\mathbf{r}$  at  $t$  because of the polarization terms involved. In such case, we regard the negative electron (hole) density as positive hole (electron) density [16].

### 3. Model systems, results and discussion

We consider a H<sub>2</sub> monomer with an equilibrium bond distance  $r_{\text{H-H}} = 0.7389 \text{ \AA}$  [16], as well as two types of dimers with the J-aggregate form having different inter-monomer distances,  $R = 0.7389 \text{ \AA}$  (equivalent to the H<sub>2</sub> bond distance) and  $3.0 \text{ \AA}$ , as simple models of strongly- and weakly-coupled aggregates, respectively. The excited states are calculated by the SCI/STO-3G level of approximation with full singly excited configurations. The excita-

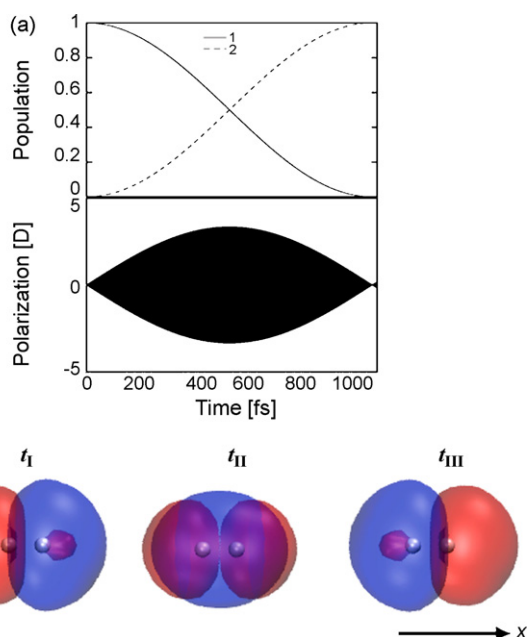


**Fig. 1.** Time evolution of diagonal density matrices,  $\rho_{11}(t)$  and  $\rho_{22}(t)$ , in the SCI state basis and polarization,  $P^x(t)$ , (a) in the presence of a cw laser field (with a power of  $100 \text{ MW/cm}^2$  and a frequency  $\omega = 208415 \text{ cm}^{-1}$ ) for H<sub>2</sub> monomer. Electron/hole (red/blue iso-surface with  $+0.001 \text{ a.u.}$ ) density distributions,  $\rho_{\text{elec}}(\mathbf{r}, t)$  and  $\rho_{\text{hole}}(\mathbf{r}, t)$ , at  $t_I = 540.523 \text{ fs}$ ,  $t_{II} = 540.563 \text{ fs}$ , and  $t_{III} = 540.603 \text{ fs}$  are shown with a coordinate axis, (b).

tion energy  $E_2$  and the transition moment  $\mu_{12}^x$  for the first dipole allowed excited state are summarized in Table 1.

Firstly we consider the monomer system. We apply a continuous wave (cw) laser with a power of 100 MW/cm<sup>2</sup>, a polarization vector along the bond axis (x-axis) and a frequency in resonance with the first dipole allowed excited state for each system. The time evolutions of the ground and excited state populations,  $\rho_{11}(t)$  and  $\rho_{22}(t)$ , in the SCI state basis as well as of x-axis component of polarization  $P^x(t)$  are shown in Fig. 1a. The  $\rho_{11}(t)$  and  $\rho_{22}(t)$  exhibit Rabi oscillations, and the oscillatory amplitude of  $P^x(t)$  is shown to increase with increasing  $t$  and to attain the maximum, where the system lies in the superposition state composed of 50% ground and 50% first excited states. The electron [ $\rho_{\text{elec}}(\mathbf{r}, t)$ ] and hole [ $\rho_{\text{hole}}(\mathbf{r}, t)$ ] densities around the times giving positive ( $t_I$ ) and negative ( $t_{III}$ ) extrema of  $P^x(t)$  as well as around at the middle time ( $t_{II}$ ) are shown in Fig. 1b. We observe the spatially asymmetric oscillations of  $\rho_{\text{elec}}(\mathbf{r}, t)$  and  $\rho_{\text{hole}}(\mathbf{r}, t)$  around the center of H<sub>2</sub> molecule, leading to the dynamic polarization in the direction of bond axis. The distributions of  $\rho_{\text{elec}}(\mathbf{r}, t)$  and  $\rho_{\text{hole}}(\mathbf{r}, t)$  at  $t_{II}$ , primarily described by the first terms of Eqs. (3) and (4), are dominated by those of LUMO and HOMO, respectively.

Second, we investigate the dimer systems in order to discuss the applicability of the present method to the J-type aggregates. We compare the dimer results calculated by the SCI method with those by the coupled dipole approximation and the SDTQ(full)-CI method (Table 1). The SCI monomer parameters,  $E_2$  and  $\mu_{12}^x$ , are employed for the calculation in the coupled dipole approximation. The HOMO and LUMO distributions are shown in Fig. 2a. For the weakly coupled model ( $R=3.0$  Å), the inter-monomer distance of 3.0 Å is large enough compared to the size of H<sub>2</sub> monomer. Judging from the shapes of HOMO and LUMO of this system, the orbital overlaps of the monomer MOs are negligible. Therefore, the Coulomb interaction is predicted to be dominant in the inter-monomer interaction. Indeed, the results of this model obtained by the coupled dipole approximation are in good agreement with the SCI results. It is noted that 97.6% and 97.0% of  $E_2$  by the full-CI method are achieved

by using the SCI method and the coupled dipole approximation, respectively.

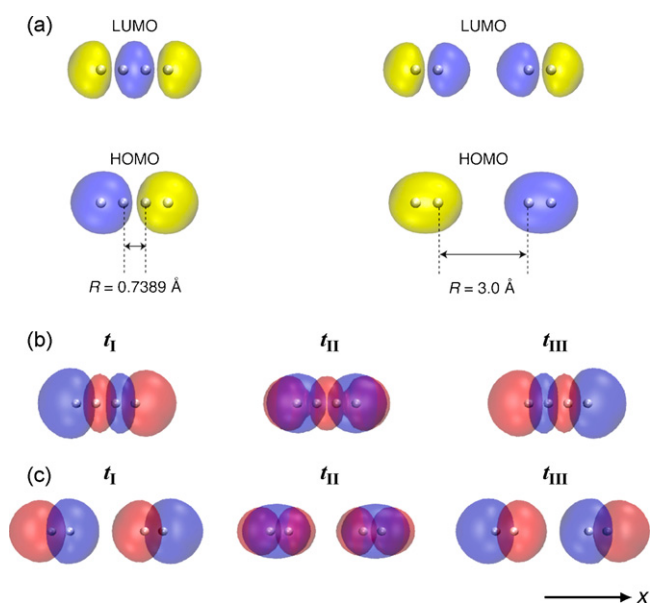
On the other hand, the coupled dipole approximation is apparently invalid for the strongly coupled model ( $R=0.7389$  Å) owing to the significant overlap of wavefunctions of monomers (see Fig. 2a). There are strong bonding interaction between the monomers, i.e., the delocalized and bonding (node-less) characters over the middle two H atoms in LUMO distribution (see Fig. 2a). Even in this case, the SCI transition energy amounts to 97.4 % of the full-CI result though it should be dependent on the choice of basis set. From the comparison of CI coefficients calculated by the SCI and full-CI methods, the HOMO-LUMO single electron excitation is dominant in the first allowed excited state. Thus, the MOQME approach based on the SCI method is expected to be applied to the exciton dynamics of systems having low-lying excited states primarily described by the single excitation configurations.

Fig. 2b and c shows electron [ $\rho_{\text{elec}}(\mathbf{r}, t)$ ]-hole [ $\rho_{\text{hole}}(\mathbf{r}, t)$ ] densities around the times giving positive ( $t_I$ ) and negative ( $t_{III}$ ) maximum amplitudes of  $P^x(t)$  as well as those at the middle time ( $t_{II}$ ) for H<sub>2</sub> dimers with  $R=0.7389$  Å and 3.0 Å, respectively. The electron and hole density distributions of the dimer with  $R=0.7389$  Å are shown to be significantly different from those of monomer. It is found at the middle time ( $t_{II}$ ) that the polarization amplitude is almost zero, which means that the off-diagonal density matrices are negligible, while the diagonal density  $\rho_{22}$  (associated with HOMO-LUMO excitation) is dominant. For both models, therefore, the spatial distributions of  $\rho_{\text{elec}}(\mathbf{r}, t)$  and  $\rho_{\text{hole}}(\mathbf{r}, t)$  reflect those of LUMO and HOMO, respectively, since the first terms of Eqs. (3) and (4) mainly contribute to  $\rho_{\text{elec}}(\mathbf{r}, t)$  and  $\rho_{\text{hole}}(\mathbf{r}, t)$ , respectively. At times  $t_I$  and  $t_{III}$ , the off-diagonal density matrices, in particular,  $\rho_{12}$ , becomes significant, so that the  $\rho_{\text{elec}}(\mathbf{r}, t)$  and  $\rho_{\text{hole}}(\mathbf{r}, t)$  distributions are well characterized by the product of HOMO and LUMO wavefunction, i.e., transition density between HOMO and LUMO (see Fig. 2).

For the model with  $R=0.7389$  Å,  $\rho_{\text{elec}}(\mathbf{r}, t)$  and  $\rho_{\text{hole}}(\mathbf{r}, t)$  have more significant distributions in the both end region than in the middle region of the dimers, indicating that the alternate oscillation of electron and hole distributions occurs between the both-end sites. This is caused by the significant field-induced virtual charge transfer between the both-end sites (see Fig. 2b), which originates in the strong covalent character of inter-monomer interaction in the first excited state reflecting the delocalized character of LUMO distribution (see Fig. 2a). As the distance  $R$  increases, such both-end oscillations due to the field-induced charge transfer disappear, and then the oscillations for each monomer become similar to those of isolated monomer (see Figs. Fig. 1b and Fig. 2c). The present results show that the increase in the inter-monomer interaction, i.e., the decrease in the inter-monomer distance, induces the coherent exciton dynamics extended over the monomers.

#### 4. Summary

Using a novel expression of electron and hole densities based on the polarization density calculated by the ab initio MO SCI method, we have examined the exciton dynamics of H<sub>2</sub> monomer and dimers with different inter-monomer distances. The present approach is found to be applicable to the exciton dynamics of strongly coupled H<sub>2</sub> dimer, which cannot be qualitatively described in the coupled dipole approximation, as well as of the weakly coupled H<sub>2</sub> dimer. The alternate electron and hole density oscillations over the monomers are observed in case of small inter-monomer distance ( $R=0.7389$  Å). This originates in the covalent character of inter-monomer interaction in the first excited state, i.e., delocalized character of LUMO distribution. Detailed discussions on the validity of this approach in several strongly coupled molecular aggregates will be required in connection with the choice of basis set and electron correlation method. The MOQME approach is now devel-



**Fig. 2.** HOMO and LUMO (yellow/blue iso-surface with  $\pm 0.05$  a.u.) spatial distributions for J-type H<sub>2</sub> dimer model with inter-monomer distance  $R=0.7389$  Å and  $R=3.0$  Å, (a), electron/hole (red/blue iso-surface with  $+0.001$  a.u.) density distributions,  $\rho_{\text{elec}}(\mathbf{r}, t)$  and  $\rho_{\text{hole}}(\mathbf{r}, t)$ , at  $t_I = 338.870$  fs,  $t_{II} = 338.925$  fs, and  $t_{III} = 338.981$  fs for J-type H<sub>2</sub> dimer model with inter-monomer distance,  $R=0.7389$  Å, (b), and at  $t_I = 383.908$  fs,  $t_{II} = 383.948$  fs, and  $t_{III} = 383.989$  fs for  $R=3.0$  Å, (c) are shown with a coordinate axis.

oped by combining with the spin-unrestricted based ab initio MO, multi-electron excitation CI, and the time-dependent density functional theory (TDDFT) methods. Such extensions of this approach are expected to be a powerful tools for the exciton dynamics of a variety of systems including open-shell conjugated molecules with various charged and spin states.

## Acknowledgments

This work is supported by Grant-in-Aid for Scientific Research (Nos. 18350007 and 20655003) from Japan Society for the Promotion of Science (JSPS), Grant-in-Aid for Scientific Research on Priority Areas (No. 18066010) from the Ministry of Education, Science, Sports and Culture of Japan, and the global COE (center of excellence) program “Global Education and Research Center for Bio-Environmental Chemistry” of Osaka University.

## References

- [1] C. Devadoss, P. Bharathi, J.S. Moore, *J. Am. Chem. Soc.* 118 (1996) 9635.
- [2] F.C. Spano, S. Mukamel, *Phys. Rev. A* 40 (1989) 5783.
- [3] S. Tretiak, V. Chernyak, S. Mukamel, *J. Phys. Chem. B* 102 (1998) 3310.
- [4] Y.R. Kim, P. Share, M. Pereira, M. Sarisky, R.M. Hochstrasser, *J. Chem. Phys.* 91 (1989) 7557.
- [5] F. Zhu, C. Grall, R.M. Hochstrasser, *J. Chem. Phys.* 98 (1993) 1042.
- [6] I. Yamazaki, S. Akimoto, T. Yamazaki, S.-I. Sato, Y. Sakata, *J. Phys. Chem. A* 106 (2002) 2122.
- [7] I. Yamazaki, N. Aratani, S. Akimoto, T. Yamazaki, A. Osuka, *J. Am. Chem. Soc.* 125 (2003) 7192.
- [8] I. Yamazaki, S. Akimoto, N. Aratani, A. Osuka, *Bull. Chem. Soc. Jpn.* 77 (2004) 1959.
- [9] T. Förster, *Discuss. Faraday Soc.* 27 (1959) 7.
- [10] H. Harigaya, *Phys. Chem. Chem. Phys.* 1 (1999) 1687.
- [11] M. Nakano, M. Takahata, H. Fujita, S. Kiribayashi, K. Yamaguchi, *Chem. Phys. Lett.* 323 (2000) 249.
- [12] M. Takahata, M. Nakano, H. Fujita, K. Yamaguchi, *Chem. Phys. Lett.* 363 (2002) 422.
- [13] M. Nakano, M. Takahata, S. Yamada, R. Kishi, T. Nitta, K. Yamaguchi, *J. Chem. Phys.* 120 (2004) 2359.
- [14] H. Nitta, M. Shoji, M. Takahata, M. Nakano, D. Yamaki, K. Yamaguchi, *J. Photochem. Photobiol. A: Chem.* 178 (2006) 264.
- [15] M. Nakano, S. Ohta, R. Kishi, M. Nate, H. Takahashi, S.-I. Furukawa, H. Nitta, K. Yamaguchi, *J. Chem. Phys.* 125 (2006) 234707.
- [16] M. Nakano, R. Kishi, T. Minami, H. Fukui, H. Nagai, K. Yoneda, H. Takahashi, *Chem. Phys. Lett.* 460 (2008) 370.
- [17] H. Haken, *Quantenfeldtheorie des Festkörpers*, B.G. Teubner, Stuttgart, 1973.
- [18] V. Czikkely, H.D. Forsterling, H. Kuhn, *Chem. Phys. Lett.* 6 (1970) 207.
- [19] C. Ecoffet, D. Markovitsi, P. Millié, J.P. Lemaistre, *Chem. Phys.* 177 (1993) 629.
- [20] D. Markovitsi, A. Germain, P. Millié, P. Lécuyert, L.K. Gallos, P. Argyrakakis, H. Bengss, H. Ringsdorf, *J. Phys. Chem.* 99 (1995) 1005.
- [21] D. Beljonne, J. Cornil, R. Silbey, P. Millié, J.L. Brédas, *J. Chem. Phys.* 112 (2000) 4749.
- [22] E. Hennebicq, C. Deleener, J.L. Brédas, G.D. Scholes, D. Beljonne, *J. Chem. Phys.* 125 (2006) 054901.
- [23] K. Fujimoto, W. Yang, *J. Chem. Phys.* 129 (2008) 054102.
- [24] M. J. Frisch et al., *Gaussian 03 Revision D.01*, Gaussian, Inc., Wallingford CT, 2004.
- [25] H.J. Carmichael, *Statistical Methods in Quantum Optics 1*, Springer, Verlag, Berlin, 1999.